

RELATIONSHIP BETWEEN EARTHQUAKE GROUND MOTION INTENSITY MEASURES AND EMBANKMENT DAM DEFORMATIONS

Richard J. Armstrong

Department of Civil Engineering
California State University, Sacramento

Abstract

The relationship between earthquake ground motion characteristics and embankment dam deformations is currently being investigated through a ground motion study using two validated non-linear deformation (NDA) embankment models. Presented in this paper are: (1) NDA results for one of the dams in this study, Lenihan Dam, against the 1989 Loma Prieta earthquake, and (2) current results of the ground motion study with this NDA model. The paper ends with major conclusions and plans for future work.

Introduction

In a seismic hazard assessment of an embankment dam, the ground motion intensity measure deemed important to the dam must first be identified (e.g., spectral acceleration, SA ; peak ground velocity, PGV ; and arias intensity, AI). Following this identification, the potential distribution of each intensity measure can be predicted using ground motion prediction equations. The actual design target level of one or more of these intensity measures can then be determined through deterministic or probabilistic seismic hazard analyses. One method of setting the design target level is the conditional mean approach, which is described in detail for use in dam engineering by Armstrong (2017). In this approach, a single intensity measure that relates well to embankment-dam response—called the conditioning intensity, IM^* —is selected, and the value is set based on the hazard level defined. The values of the other intensity measure targets are then selected according to the value of this conditioning intensity measure and other statistical considerations. When the conditional mean approach is used, it is important for the conditioning intensity measure, IM^* , to relate well to the engineering demand parameter (EDP) of interest—for example, vertical crest deformation—because the expectation is that as IM^* increases, so should the EDP . More specifically, as stated by Kramer (2008), IM^* should be unbiased, consistent, robust, efficient, and sufficient.

Previous studies have investigated the relationship between ground motion intensity measures and embankment or slope deformation. Based on these studies, it has been suggested that for stiff embankment dams in which significant strength loss is not expected, the SA at the first-mode period of the structure relates well with embankment deformations. However, for embankment dams founded on liquefiable alluvium, other non- SA intensity measures have been found to relate better to embankment deformations (Beaty and Perlea 2012)—such as AI ; cumulative absolute velocity, CAV ; and $\sqrt{AI \cdot D595}$, where $D595$ is the duration between 5% and 95% AI . These studies, however, have been based on relatively simplified Newmark-type

sliding block analyses with large ground motion databases (e.g., Bray and Travasarou 2007, Saygili and Rathje 2007) or on non-linear deformation analyses shaken with significantly smaller sets of ground motions (Beaty and Perlea 2012).

In a current project—supported by the California Department of Conservation, California Geological Survey, Strong Motion Instrumentation Program, Agreement 1016-988—data from strong ground motion recordings from two embankment dams during the 1989 Loma Prieta earthquake are being used to validate each non-linear deformation analysis model for subsequent use in assessing the relationship between earthquake ground motion characteristics and embankment dam deformations. Currently, a suite of over 700 ground motions is being used in this assessment. It is anticipated that at the completion of this project, this work will provide significant additional insight into the relationship between ground motion characteristics and embankment dam deformations.

The purpose of this paper is twofold: (1) to present NDA results for one of the dams in this study, Lenihan Dam, against the 1989 Loma Prieta earthquake, and (2) to present current results of the ground motion study with this NDA model. The paper will begin with a detailed description of the validation of the NDA of Lenihan Dam to the 1989 Loma Prieta earthquake, followed by a description of the ground motion database used and an initial evaluation of the results. The paper will end with conclusions and plans for future work.

Background

Lenihan Dam

James J. Lenihan Dam (or, simply, Lenihan Dam, which is sometimes called Lexington Dam) is a zoned earthfill dam that was constructed across Los Gatos Creek in 1952 (Figures 1 and 2). The dam impounds Lexington Reservoir, which has a maximum capacity of 19,044 acre-feet at the spillway elevation of 653 feet (TGP 2012). The crest of the dam is at elevation 673 feet, with an embankment height of 195 feet measured from the lowest point of the foundation rock to an embankment height of 207 feet measured from the lowest point of the downstream toe. The zoned earthfill dam is composed of upstream and downstream shells, core, and drainage zones. The core is further divided into an upper and lower core to reflect differences in material properties. The upstream shell and upper core material were obtained from the same borrow source. The upstream shell is generally composed of gravelly clayey sands to sandy clays, while the upper core is composed of gravelly clayey sand to clayey gravel. The lower core came from another borrow source with the material being generally classified as highly plastic sandy clays to highly plastic silty sands-sandy silts. The downstream shell, obtained from a third borrow source, consists mainly of gravelly clayey sand to clayey gravels. No classification information is available for the drain material. The embankment materials were constructed on Franciscan Complex bedrock, without a foundation seepage cutoff or grout curtain. Instrumentation of Lenihan Dam includes survey monuments, piezometers, inclinometers, seepage weir, and strong ground motion accelerometers.

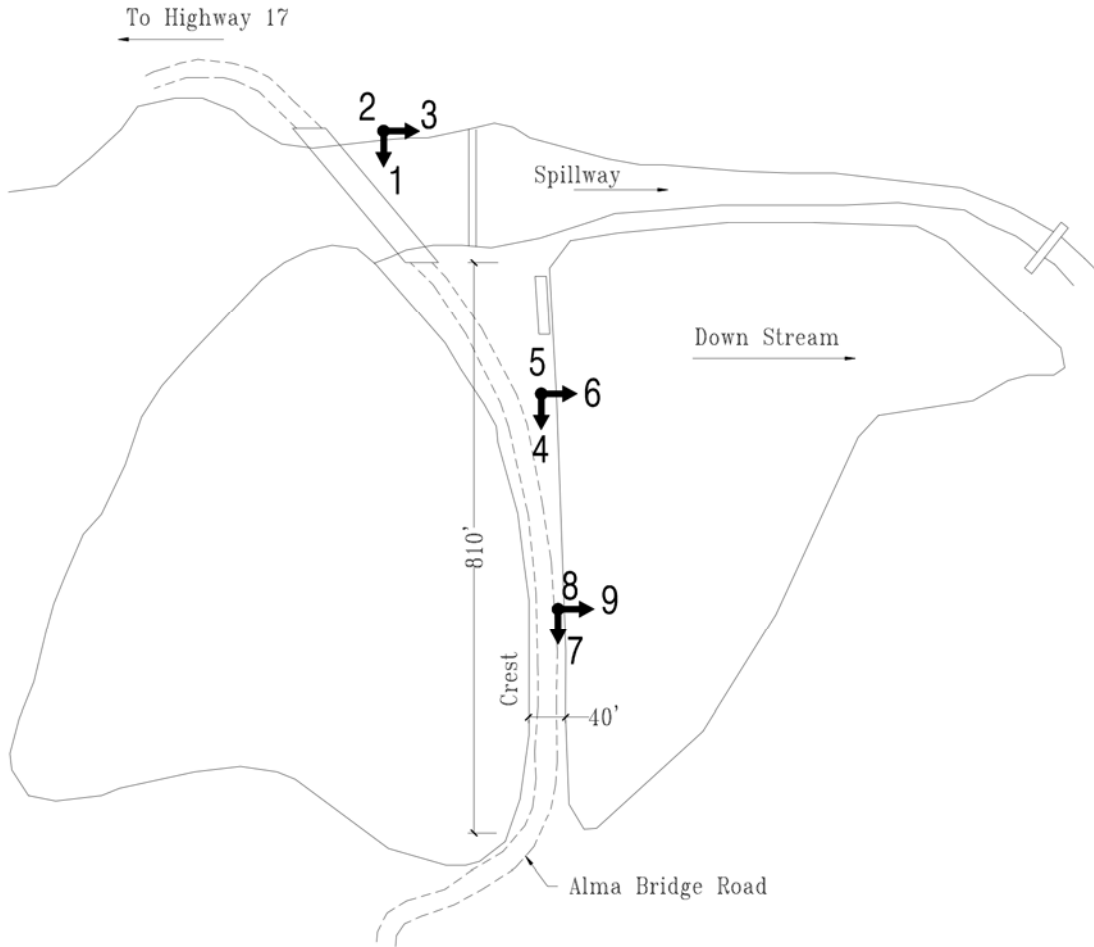


Figure 1. Plan view of Lenihan Dam with locations of strong motion instruments (from Center for Earthquake Strong Ground Motion).

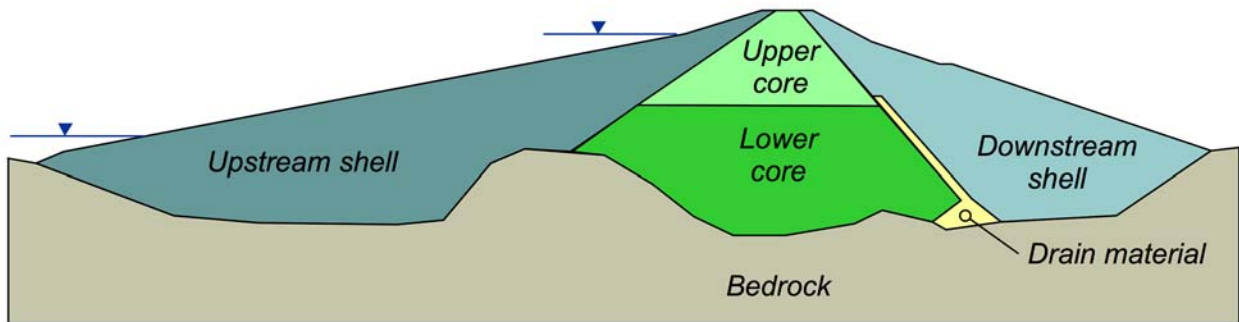


Figure 2: Design cross-section with reservoir level of 556 feet during the 1989 Loma Prieta Earthquake and at the spillway elevation of 653 feet.

Loma Prieta Earthquake

The $M = 6.9$ Loma Prieta earthquake occurred along a segment of the San Andres fault on October 17, 1989. The epicenter of this earthquake event was located 13 miles from Lenihan Dam. At the time of the earthquake, the reservoir was at around elevation 556 feet – 97 feet below the spillway. During this earthquake, strong ground motion instruments located at the left abutment and on the crest measured the dynamic response of the dam. Due to the strong shaking, the embankment crest deformed horizontally around 3 inches downstream and approximately 10 inches vertically downward, resulting in longitudinal and transverse cracking at the dam site (Hadidi et al. 2014).

Analysis of the strong ground motion data is provided in Figure 3 in terms of the SA , ratio of the crest SA to abutment SA , peak ground velocity (PGV), AI , and $D595$. The results shown in Figure 3 correspond to the strong ground motion recording in the transverse directions (directions “3”, “6”, and “9” in Figure 1). Peak ground acceleration (PGA) changed from 0.44g at the abutment to between 0.38g and 0.45g along the crest. The most significant increase in acceleration corresponded to a spectral period of 1 second, which roughly represents the natural period of the dam.

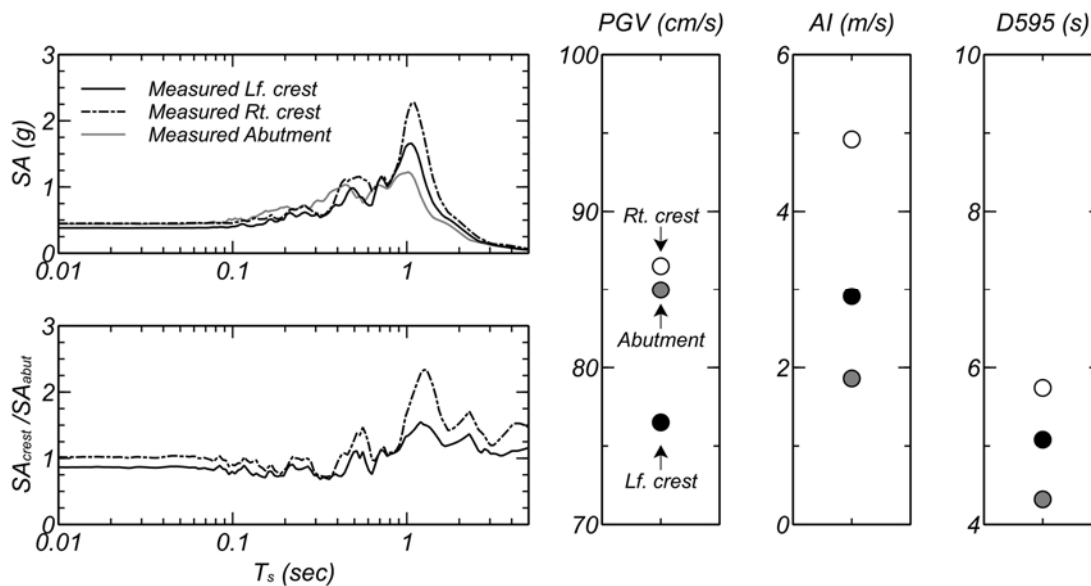


Figure 3: Measured ground motion characteristics in transverse direction during the 1989 Loma Prieta earthquake.

Non-linear Deformation Analysis of Lenihan Dam

Analysis Approach

Numerical Analysis Details

The NDA was conducted using the commercial program FLAC (Itasca Consulting Group, 2016). This program uses an explicit solution scheme and is well suited for performing deformation analyses with non-linear material response, large geometry changes, and instability. The explicit solution satisfies the equations of motion at each nodal mass for every time step. The numerical mesh used in the NDA is shown in Figure 1. The element size was selected to accurately transmit motion frequencies up to at least 10 hertz.

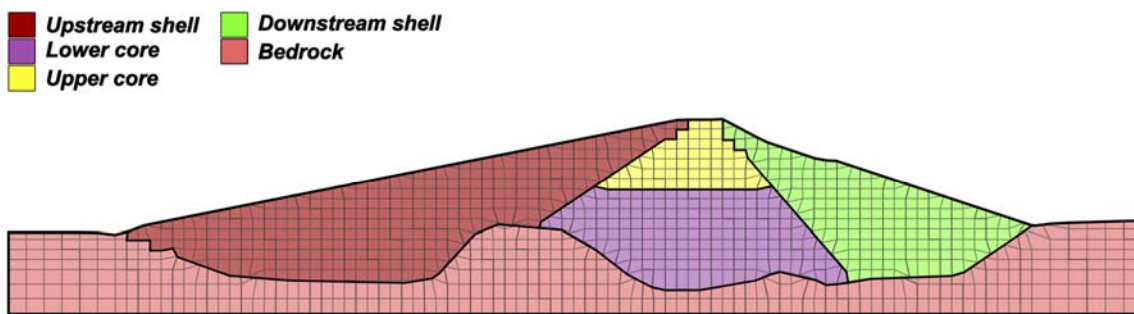


Figure 4: Numerical mesh.

Constitutive Modeling Approach

The UBCHYST constitutive model (Byrne and Naesgaard, 2011) was used to model the expected non-linear soil response during the 1989 Loma Prieta earthquake. The UBCHYST model captures, with increased shear strain, the reduction of shear modulus and increase in hysteretic damping. The UBCHYST is essentially an extension of the Mohr-Coulomb model with a tangent shear modulus that is a function of the developed stress ratio and other modification factors. Up to 11 input parameters can be set to control various aspects of the UBCHYST constitutive model response. Of those 11 input parameters, the following five parameters were modified in these analyses: maximum shear modulus (G_{max}) and bulk modulus, cohesion (S), hysteretic parameter (n), and hysteretic parameter (R_f). The first three input parameters are also inputs into the elastic-perfectly plastic Mohr-Coulomb model, while the last two input parameters help to define the hysteretic behavior of UBCHYST. Of n and R_f , n was found to have the most significant effect on the hysteretic behavior. As a result, R_f was simply set to the recommended default value of 0.98, and n was used to adjust the constitutive model response to capture the desired dynamic soil element behavior. In particular, the expected dynamic soil behavior was defined through the G/G_{max} and ξ curves developed by Vucedic and Dobry 1991 (termed here VD91).

The input parameter n was selected by comparing the calculated G/G_{max} and ξ of single element simple shear simulations to those values from VD91. In performing these simulations, it

was found that n as well as the ratio of the shear strength to maximum shear modulus (S/G_{max}) both significantly affect the calculated value of G/G_{max} and ξ . Because the goal was to have a single target G/G_{max} and ξ for each material in the embankment, and S/G_{max} will change throughout the embankment, it was then necessary to define a relationship between n and S/G_{max} . To accomplish this, a large suite of single element simple shear simulations was conducted with UBCHYST, with varying values of n and S/G_{max} ; further, a statistical relationship was developed between n and S/G_{max} so that all numerical elements, regardless of S/G_{max} , would result in the same target curve from VC91. Specifically, it was found that for the target shear modulus and damping curves from $PI = 15$ and $PI = 30$ used in VC91, the necessary relationship between n and S/G_{max} was $n = 2300 \times S/G_{max}$ for $PI = 15$ and $n = 1300 \times S/G_{max}$ for $PI = 30$.

An example of the dynamic simple shear response of UBCHYST using this technique is shown in Figure 5. For this example, the ratio between the S to G_{max} was 8×10^{-4} , a range consistent with the NDA model of the embankment. To reasonably match the VD91 for $PI = 30$, for example, $n = 1.04$. As highlighted in Figure 5, UBCHYST is capable of matching the G/G_{max} curve up to around a shear strain of 0.001, after which the reduction in G/G_{max} is over-predicted. For the ξ curve, the UBCHYST model is able to match the curve up to a shear strain of approximately 0.0002, after which the model predicts hysteretic damping significantly larger than what would be expected from VD91. The highlighted shortcomings of UBCHYST are primarily due to its basis on the Mohr-Coulomb model formulation.

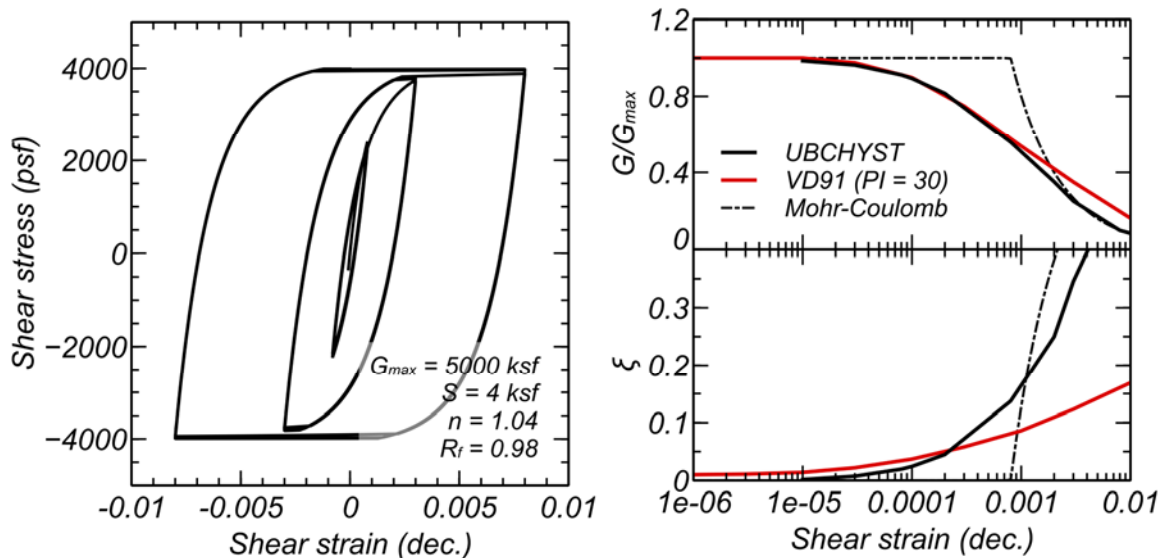


Figure 5. Stress-strain and resulting G/G_{max} and ξ curves for UBCHYST. Comparison to Vucedic and Dobry 1991 (VD91) with $PI = 30$ and the Mohr-Coulomb model.

Material Property Characterization

Over the years, multiple site investigation programs have been conducted at Lenihan Dam. The most recent such program took place in 2012 by TGP (TGP, 2012). When defining material properties based on this site investigation information, the material characterization completed by TGP and summarized in the work by Hadidi et al. 2014 was used extensively to define material properties. The primary difference between the material properties found here and those used by Hadidi et al. 2014 was the modeling of the variation of shear strength with effective stress. In this work, the shear strength was defined as $S = b' + \sigma' \tan \beta'$ for drained strength and $S = b + \sigma' \tan \beta$ for undrained strengths where $\sigma' = (\sigma'_x + \sigma'_y)/2$, with the values of intercepts and slopes defined in Table 1 below. These strength envelopes are based directly on the triaxial strength data.

Based on geophysical investigation data, the variation in G_{max} was defined in terms of the vertical effective stress (σ'_y) at 1 atm, V_{s1} , and the exponent m with $G_{max} = \rho V_s^2 = \rho \times ((V_{s1}/\sigma'_y)^m)^2$. Note that the rock beneath the soil embankment had a $\gamma = 140$ psf, $V_s = 4500$ ft/s. The value of n from the UBCHYST model was determined to match the target G/G_{max} and ξ curve for VD91 with a $PI = 30$ for the lower core, and the target G/G_{max} and ξ curve for VD91 with a $PI = 15$ for all other embankment soils. A small proportion of Rayleigh damping was included for the embankment material and rock to capture small strain damping characteristics as well as to reduce numerical noise.

Table 1. Key material parameters used in NDA

Parameters	Upstream shell	Downstream shell	Upper core	Lower core
γ (psf)	138	140	132	124
V_{s1} (ft/s)	1305	1550	1190	680
m	0.5			
β' (deg.)	31.3	29.8	30.1	23.3
b' (psf)	50		0	
β (deg.)	28.8	18.8	27.9	19.3
b (psf)	1020	1570	960	1090
R_f	0.98			
$n^{(A)}$	$2300 \times S/G_{max}$			$1300 \times S/G_{max}$

Notes (A): variation n defined for lower core chosen to match G/G_{max} and ξ curve for $PI = 30$ from VD91, and variation of n for other embankment material chosen to match G/G_{max} and ξ curve for $PI = 15$ from VD91.

Establishment of Pre-earthquake Stresses and Boundary Conditions

The pre-earthquake state-of-stress affects both initial conditions for the dynamic analysis and the value of shear strength, which is a function of the effective stress. Total stresses for the embankment were estimated by sequentially adding rows of elements of the mesh and solving for static equilibrium with each new row of elements. This process was continued for the entire embankment. The goal of this process was to roughly mimic the actual construction process.

A seepage analysis was used to model the pore water pressures in the embankment immediately before the 1989 Loma Prieta earthquake. Note that prior to the 1989 Loma Prieta earthquake, several years of below-average rainfall occurred. This resulted in a reservoir level of 506 feet, significant lower than the spillway elevation of 653 feet. Due to the low permeabilities in the embankment, the pore water pressure would slowly respond to this lower reservoir level. Modeling this non-steady state seepage condition could not be achieved using a steady-state seepage analysis with the reservoir at the level of either 506 feet or 653 feet.

In an attempt to reasonably model these non-steady state seepage conditions, the approach used was first to model the steady-state seepage conditions corresponding to the reservoir of 653 feet, and then to lower the reservoir to 506 feet and rerun the analysis until the pore water pressure in the embankment was lowered to the values similar to those measured prior to the 1989 Loma Prieta earthquake. For the initial steady-state seepage conditions corresponding to the reservoir at 653 feet, values of the horizontal and vertical permeability were adjusted until the calculated total head reasonably corresponded to values measured at Lenihan Dam for the piezometer recordings when the reservoir was near the same elevation. Note that the piezometer reading used to evaluate the reasonableness of the non-steady state seepage analysis with the reservoir at 506 feet were based both on actual piezometer readings at the time of the 1989 Loma Prieta earthquake (represented by blue square symbols in Figure 6) and on recent piezometer readings with a previous reservoir response similar to that which occurred before the 1989 Loma Prieta earthquake. Specifically, the piezometer readings from December 2008 were seen to have a previous reservoir response as before the 1989 Loma Prieta earthquake, and the piezometer data from this time was used (represented by blue circle symbols in Figure 6). As seen in Figure 6, by comparison of the calculated and total heads, the seepage model was able to reasonably capture the distribution of total heads.

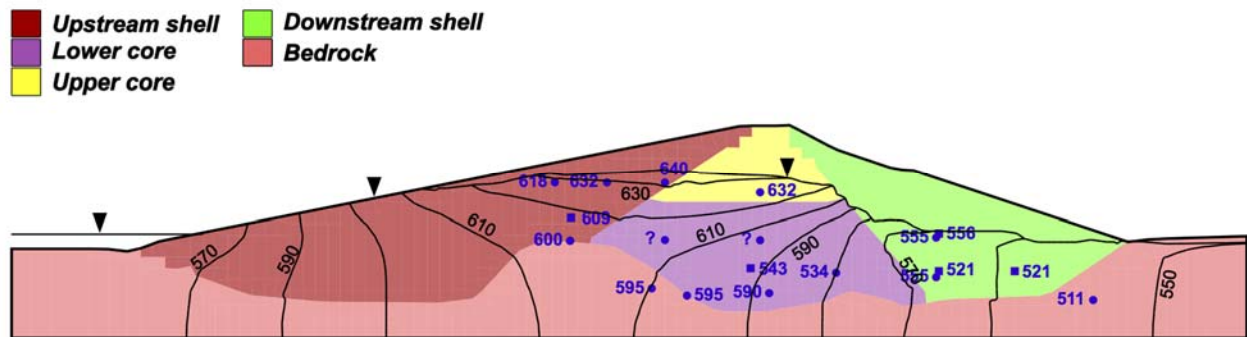


Figure 6. Comparison of calculated and target total heads.

Dynamic Analysis Results

Dynamic analyses were conducted with the transverse acceleration time history from the 1989 Loma Prieta earthquake applied directly at the base of the numerical model. To model the elastic half space below the numerical model, numerical dashpots are added and the velocity time history of the abutment record is converted to a shear stress time history based on the stiffness properties of the rock.

As an initial evaluation of the NDA results, the calculated and measured time histories are shown in Fig. 7 in terms of the SA at the crest, the ratio of the crest SA to abutment SA , and the PGV , AI , and $D595$ computed at the crest. As highlighted by these results, the NDA was able to capture reasonably well key aspects of the observed site response (e.g., SA_{crest}/SA_{abut}) as well as other peak response characteristics (PGA , PGV , and AI) and duration ($D595$).

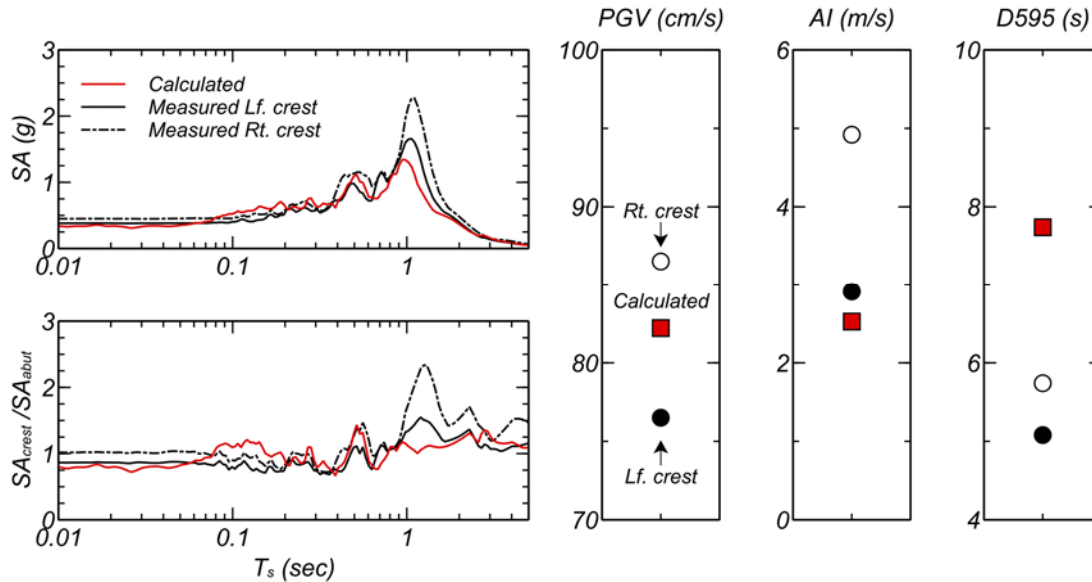


Figure 7: Summary of the calculated and measured dynamic responses at the embankment crest.

In terms of computed deformations, the final crest displacements computed with the NDA were similar to those measured. In particular, the final horizontal displacement (DXF) was 0.27 feet, compared to the measured horizontal displacement between 0.10 and 0.25 feet; and the final vertical displacement (DYF) computed was 0.45 feet, compared to the 0.61 to 0.85 feet measured.

The computed distribution of the shear strains is shown in Fig. 9(a) in terms of the shear strain increment defined as $\frac{1}{2}\sqrt{(\epsilon_x - \epsilon_y)^2 + 4\epsilon_{xy}^2}$. Localized areas of high shear strain increment are shown in both the upstream and downstream shells, producing the typical circular-type localized failure surfaces expected with slope instability. The computed distributions of horizontal and vertical displacement are shown in Figures 9(c) and (d), respectively, and are relatively consistent with the pattern of deformations and cracks observed. For example, the region where DXF changes from positive to negative corresponded to high volumetric strain extension (Figure 9(b)) and corresponded directly to the location of longitudinal cracking observed following the Loma Prieta earthquake.

Overall, the NDA was able to reasonably capture the dynamic characteristics from the 1989 Loma Prieta earthquake as well as the magnitude and distribution of displacements. The NDA model of Lenihan dam was then used to further explore the relationship between embankment dam deformations and earthquake shaking in the ground motion study.

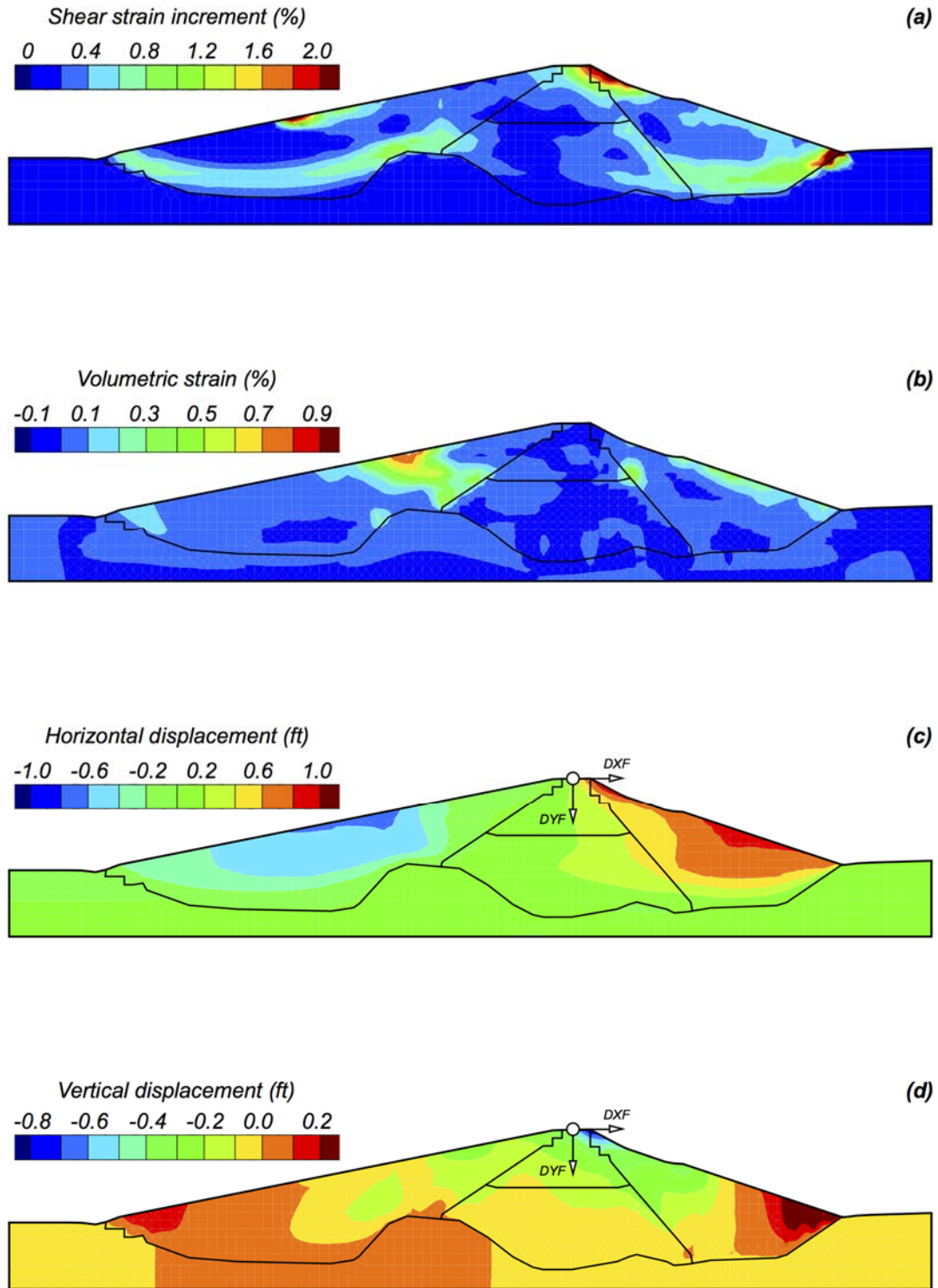


Figure 9: Computed deformations in terms of shear strain increment (a), volumetric strain (b), horizontal displacement (c), and vertical displacement (d).

Numerical Analysis Ground Motion Study

Characteristics of Ground Motion Database

The ground motion database used with the NDA model of Lenihan dam was similar to that used previously in Armstrong (2016). These ground motions were based on the NGA-West1 database with source-to-site distance less than 30 km, similar to many dams in California. For this work, only ground motions based on earthquake events with $M \geq 6$ were used, because it was expected that strong shaking for earthquake events less than 6 would not produce appreciable deformations and therefore would not be particularly useful to evaluate the relationship between embankment deformation and earthquake ground shaking characteristics. For each station, both orthogonal components of the measured strong ground motion acceleration were used if available.

A total of 716 ground motion recordings were found to satisfy this criteria, with distributions of strong ground motion intensity measures of PGA , PGV , AI , and $D595$ shown in Figure 7. Referencing the abutment motion from the 1989 Loma Prieta earthquake with a $PGA = 0.44g$, $PGV = 85.0$ cm/s, $AI = 1.86$ m/s, and $D595 = 4.32$ s, it is seen that the ground motions in this database have ground motion intensity measures that extend from less than to greater than the values measured in the Loma Prieta earthquake. Therefore, it is expected that the resulting deformation will go from negligible to values greater than those observed in the Loma Prieta earthquake. Future plans are to include ground motions from the NGA-West-2 database to augment those in this database, especially those with high ground motion intensity measure values.

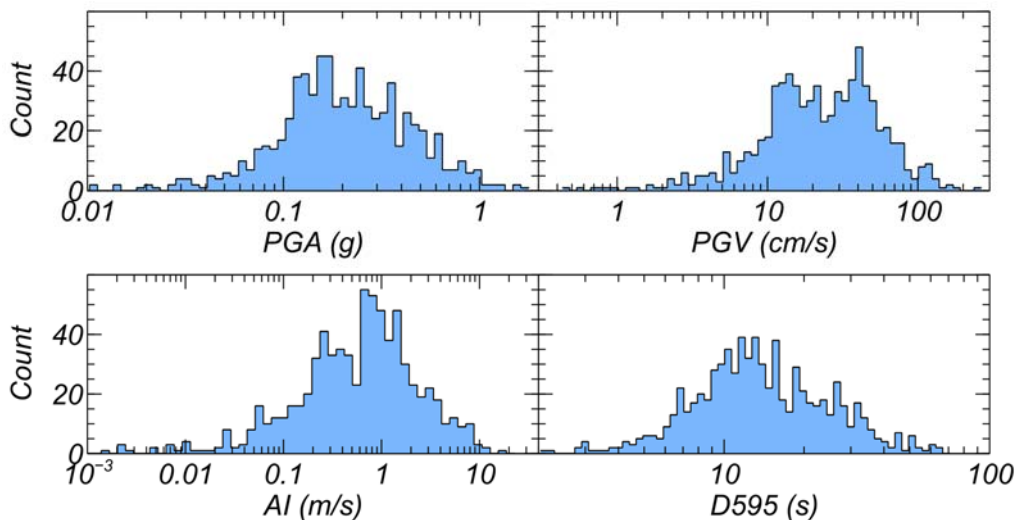


Figure 10. Distribution of ground motion intensity measures.

Numerical Analysis Results

Analyses of the NDA model of Lenihan Dam were conducted with the 716 ground motion time histories described above. The NDA model used was identical to that of Lenihan Dam, except that the reservoir level used was that for a spillway elevation of 653 feet. For each analysis, time histories at key locations were stored, as well as the final solved state of the NDA model.

In this evaluation, the trends between the ground motion intensity measures (*IMs*) at the base of the model to key engineering demand parameters (*EDP*) are compared. The ground motion intensity measures computed were *PGA*, *PGV*, *AI*, cumulative absolute velocity (*CAV*), *D595*, and *SA* at 200 equal logarithmic increments of spectral period between 0.1 and 30 seconds. The engineering demand parameters computed were peak and final horizontal crest displacement, *DXP* and *DXF*, and the peak and final vertical crest displacement, *DYP* and *DYF*. Note that in computing these displacements, the displacement was computed relative to the base of the model. Also, the absolute value of the peak and final vertical crest displacement were chosen because the logarithm would otherwise be undefined. Further, only analyses resulting in non-negligible deformation, defined here as a value of *DXP*, *DXF*, *DYP*, or *DYF* greater than 0.1 feet, were included. This reduced the NDA results to be compared from 716 to 504.

An initial evaluation of the relationships between the embankment crest deformation and ground motion intensity measures is shown in Figure 11 (note that only *SA* at a selection of spectral periods is included). In each plot, the \log_{10} of the *IM* is compared to the \log_{10} of the *EDP*. The magnitude of the *IMs* and *EDPs* have been removed for clarity in comparing plots. A linear trend line is included in each plot, as well as a density ellipse to represent visually the correlation relationship between the *IM* and *EDP*. As seen in Figure 11, the ability of each *IM* to relate to an *EDP* varies significantly. *PGA*, *AI*, and *SA* at shorter spectral periods related best to the *EDPs*. Other intensity measures—such as *PGV*, *CAV*, and *SA*—at higher spectral periods still related to the *EDPs*, but not as strongly as with *PGA*, *AI*, and *SA* at short spectral periods.

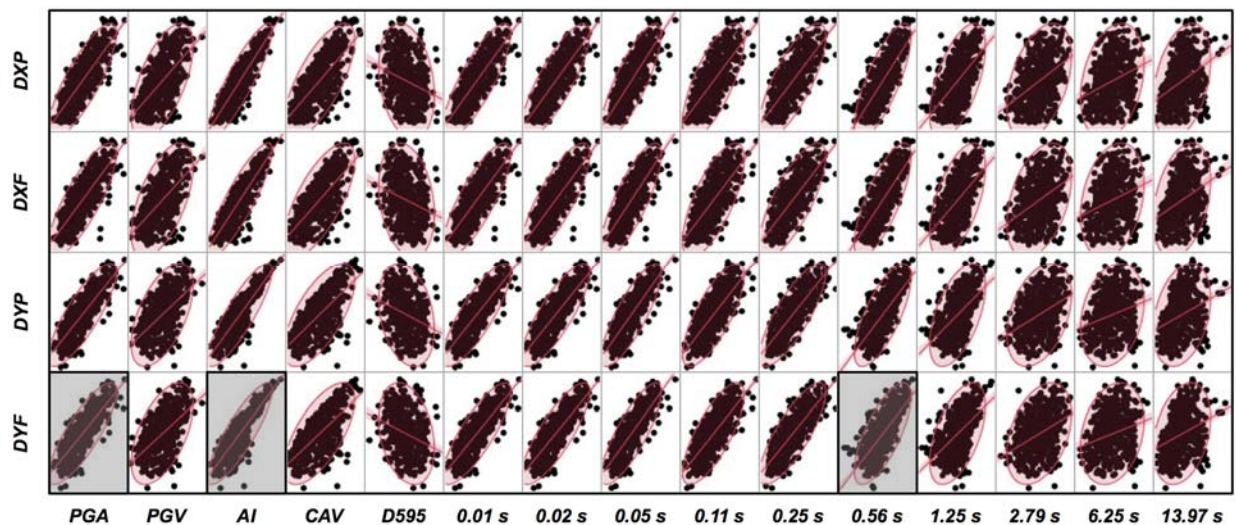


Figure 11. Comparison of *IMs* and *EDPs* (all axes are logarithmic).

A closer inspection of the relationship between AI , PGA , and $SA(0.56)$ and DYF shown in Figure 11 is provided in Figure 12. AI and PGA were chosen because AI ranked first and PGA second in order of goodness-to-fit with DYF . SA at a spectral period of 0.56 s was selected because it laid within the expected range of the period of the embankment for many of the analyses. As in Figure 11, a linear trend line is included. Also included in Figure 12 is the magnitude and distribution of DYF and each of the three IM s as well as the standard deviation from the simple bivariate regression analysis.

As highlighted in Figure 12, the relationship between AI and DYF and then PGA and DYF resulted in the lowest standard deviation; therefore, for this particular model, AI , then PGA were the most efficient prediction of this EDP. Therefore, in terms of selecting a conditioning intensity measure for the NDA model of this dam, AI appears to be the preferred IM . It is important to note that the observed relationship between embankment deformations and ground motion intensity measures here is based only on the NDA model of Lenihan Dam. Plans for additional ground motions, more detailed statistical evaluations, and a second validated NDA model will be helpful in better defining the relationship between ground motion intensity measures and embankment dam deformations.

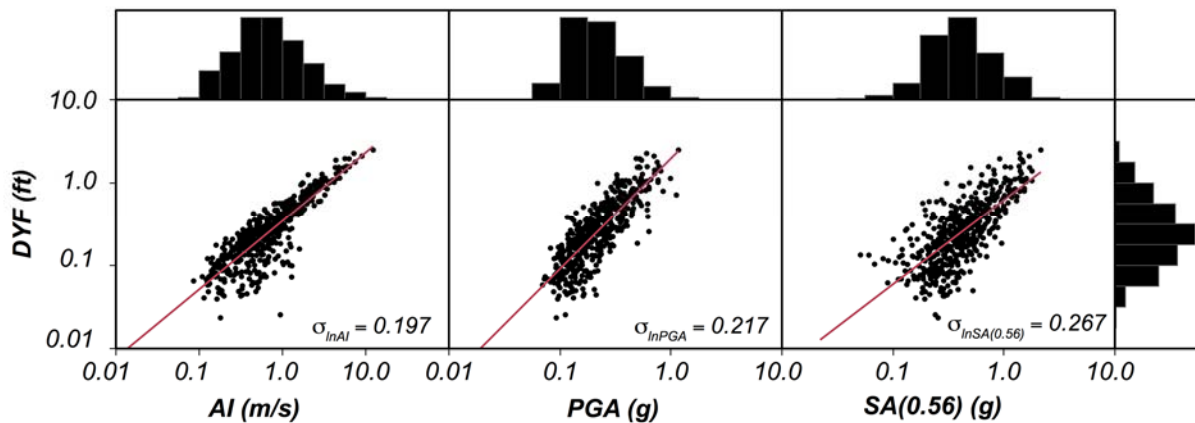


Figure 12. Comparison of intensity measures and engineering demand parameters.

Conclusions

The measured strong ground motion data at Lenihan Dam during the 1989 Loma Prieta earthquake provided a useful case-history to assess the capabilities of current NDAs. With the analysis approach described, the NDAs were able to capture reasonably well key dynamic characteristics such as the surface acceleration response spectra and the magnitude and pattern of permanent deformations. Using the NDA model for Lenihan Dam, additional analyses with the 716 ground motions provided insight into the relationship between ground motion intensity measures and embankment dam deformation. For the NDA model used, *AI* was found to relate best with embankment dam deformations, followed by *PGA* and then *SA* at short spectral periods. Plans to use additional ground motions, to perform more detailed statistical evaluations, and to include a second validated NDA model will be helpful in better defining the relationship between embankment dam deformations and ground motion intensity measures. The second NDA model to be included is of Anderson Dam. This dam was also shaken during the Loma Prieta earthquake, with multiple strong ground motion recordings available. Development of this NDA model is ongoing. Note that for Anderson Dam at the design loading earthquake levels, liquefaction of portions of the embankment and foundation material is expected; thus, this dam model will provide a useful comparison to Lenihan Dam, which had no liquefaction concerns. Ground motions from the NGA-West-2 database will be added to the database currently used and will provide improved insight into the relationship between ground motion intensity measures and embankment dam engineering demand parameters.

Acknowledgements

This work was supported by the California Department of Conservation, California Geological Survey, Strong Motion Instrumentation Program, Agreement 1016-988. The funding provided is greatly appreciated. The work and comments by Howard Yoon and Dr. Dong Soon Park as it relates to this project were particularly valuable.

References

- Armstrong R.J. (2016). Procedure for selecting and modifying earthquake motions to multiple intensity measures. *Soil Dynamics and Earthquake Engineering*. 89.
- Armstrong R.J. (2017). Use of the conditional mean for improved prediction of ground motion intensity measures for embankment dams. Proceedings, *2014 Annual United States Society of Dams Conference*.
- Beatty M.H., and Perlea V.G. (2012). Effect of ground motion characteristics on liquefaction modeling of dams. *ASCE GeoCongress*.
- Bray J.D., and Travararou T. (2007). Simplified procedure for estimating earthquake-induced deviator slope displacement. *Journal of Geotechnical and Geoenvironmental Engineering*, 133(4), 381–92.
- Byrne, P.M. and Naesgaard, E. (2010). Personal Communications. UDM Version: 5d. <https://www.itascacg.com/udms/ubchyst> (Accessed 10/16/17).

- Hadid, R., Moriwaki, Y., Barneich, J., Kirby, R., Mooers, M. (2014). Seismic deformation evaluation of Lenihan Dam under 1989 Loma Prieta Earthquake. *Tenth U.S. National Conference on Earthquake Engineering*, Frontiers of Earthquake Engineering.
- Itasca Consulting Group. (2016). FLAC, fast lagrangian analysis of continua, user's guide, version 8.0, Itasca Consulting Group, Minneapolis.
- Kramer S.L. (2008). Performance-based earthquake engineering: opportunities and implications for geotechnical engineering practice. *Geotechnical Earthquake Engineering and Soil Dynamics IV*, D. Zeng, M. Manzari, and D. Hiltunen, eds., Geotechnical Special Publication No. 181, ASCE, NY.
- Makdisi, F.I., Chang, C.Y., Wang Z.I., and Mok C.M. (1991). Analysis of the Recorded Response of Lexington Dam During Various Levels of Ground Shaking, Proc. Of the Seminar on Seismological and Engineering Implications of Recent Strong Motion data, SMIP, California Division of Mines and Geology, 1991. □
- Saygili G and Rathje E.M. (2007). Empirical predictive models for earthquake-induced sliding displacements of slopes. *Journal of Geotechnical and Geoenvironmental Engineering*, 134(6), 790–803.
- Terra / GeoPentech. (2012). Lenihan Dam, Site Characterization, Material Properties and Ground Motion (Report No. LN-3), Prepared for Santa Clara Valley Water District.
- Vucetic, M. and Dobry, R. (1991). Effect of soil plasticity on cyclic response. *Journal of Geotechnical Engineering Division*, 117(1), 89-107.

